Evaluation of Requirements for the DWPF Higher Capacity Canister

D. H. Miller
E. G. Estochen
J. M. Jordan
M. R. Kesterson
C. A. McKeel

August 2014

SRNL-STI-2012-00417

DISCLAIMER

Printed in the United States of America

Prepared for
U.S. Department of Energy

SRNL-STI-2012-00417
Revision 0

Keywords: *DWPF, Canisters*

Retention: *Permanent*

Evaluation of Requirements for the DWPF Higher Capacity Canister

D. H. Miller
E. G. Estochen
J. M. Jordan
M. R. Kesterson
C. A. McKeel

August 2014

Prepared for the U.S. Department of Energy under contract number DE-AC09-08SR22470.

Savannah River National Laboratory™
OPERATED BY SAVANNAH RIVER NUCLEAR SOLUTIONS

REVIEWS AND APPROVALS

AUTHORS:

D. H. Miller, Engineering Process Development Date

E. G. Estochen, Material Applications and Process Technology Date

J. M. Jordan, HB-Line Process Engineering Date

M. R. Kesterson, Applied Computational Engineering and Statistics Date

C. A. McKeel, Packaging Technology and Pressurized Systems Date

TECHNICAL REVIEW:

D. T. Herman, Advanced Characterization and Process Date

J. W. Amoroso, Process Technology Programs Date

APPROVAL:

E. N. Hoffman, Manager Date
Engineering Process Development

S.L. Marra, Manager Date
Environmental & Chemical Process Technology Research Programs

E. J. Freed, Manager Date
Waste Solidification Engineering

ACKNOWLEDGEMENTS

The work completed by several co-authors and contributors is highlighted in this report and also included as references. Matt Kesterson and Jeff Jordon created models comparing the thermal and stress conditions of the two canister types. Charles McKeel performed structural calculations to examine the various forces exerted on the canisters during processing. Eddie Estochen and Ken Imrich directed the environmental testing for corrosion evaluation.

EXECUTIVE SUMMARY

The Defense Waste Processing Facility (DWPF) is considering the option to increase canister glass capacity by reducing the wall thickness of the current production canister. This design has been designated as the DWPF Higher Capacity Canister (HCC). A significant decrease in the number of canisters processed during the life of the facility would be achieved if the HCC were implemented leading to a reduced overall reduction in life cycle costs. Prior to implementation of the change, Savannah River National Laboratory (SRNL) was requested to conduct an evaluation of the potential impacts. The specific areas of interest included loading and deformation of the canister during the filling process. Additionally, the effect of the reduced wall thickness on corrosion and material compatibility needed to be addressed. Finally the integrity of the canister during decontamination and other handling steps needed to be determined. The initial request regarding canister fabrication was later addressed in an alternate study.

A preliminary review of canister requirements and previous testing was conducted prior to determining the testing approach. Thermal and stress models were developed to predict the forces on the canister during the pouring and cooling process. The thermal model shows the HCC increasing and decreasing in temperature at a slightly faster rate than the original. The HCC is shown to have a 3°F ΔT between the internal and outer surfaces versus a 5°F ΔT for the original design. The stress model indicates strain values ranging from 1.9% to 2.9% for the standard canister and 2.5% to 3.1% for the HCC. These values are dependent on the glass level relative to the thickness transition between the top head and the canister wall.

This information, along with field readings, was used to set up environmental test conditions for corrosion studies. Small 304-L canisters were filled with glass and subjected to accelerated environmental testing for 3 months. No evidence of stress corrosion cracking was indicated on either the canisters or U-bend coupons.

Calculations and finite element modeling were used to determine forces over a range of handling conditions along with possible forces during decontamination. While expected reductions in some physical characteristics were found in the HCC, none were found to be significant when compared to the required values necessary to perform its intended function.

Based on this study and a review[1] of successful testing of thinner canisters at West Valley Demonstration Project (WVDP), the mechanical properties obtained with the thinner wall do not significantly undermine the ability of the canister to perform its intended function.

TABLE OF CONTENTS

LIST OF TABLES

LIST OF FIGURES

LIST OF ABBREVIATIONS

ASTM	American Society for Testing and Materials
DWPF	Defense Waste Processing Facility
FEA	Finite Element Analysis
GWSB	Glass Waste Storage Building
HCC	Higher Capacity Canister
KSI	Kilo-pound per Square Inch
MFT	Melter Feed Tank
PEEQ	Equivalent Plastic Strain
SCC	Stress Corrosion Cracking
SRNL	Savannah River National Laboratory
SRNS	Savannah River Nuclear Solutions
TTQAP	Task Technical and Quality Acceptance Plan
TTR	Technical Task Request
WAPS	Waste Acceptance Product Specifications
WSE	Waste Solidification Engineering
WVDP	West Valley Demonstration Project

1.0 Introduction

The current canister being used at the Defense Waste Processing Facility (DWPF) uses a 3/8" thick canister wall. A 10-gauge wall thickness would allow approximately 4% increased glass capacity and reduce the number of production canisters required over the life of the facility. A significant life cycle cost savings would be achieved. Since the outside diameter of the canister would remain the same, the change would be transparent to the process except for certain requirements that were based on the current design thickness. The requirements are listed in multiple sections of the DWPF Waste Form Compliance Plan[2]. These include the quality of the material, methods used for construction of the canisters and multiple performance criteria such as closure and drop tests. A Technical Task Request[3] (TTR) was issued to SRNL to evaluate the requirements of the proposed higher capacity canister. A plan was developed to address the major areas of concern and was issued in an approved Task Technical and Quality Assurance Plan[4] (TTQAP).

The task was broken down into several main areas. Along with a review of literature for applicable data, the thermal loading and deformation were modeled for a comparison between the two canister designs. Structural calculations were completed to address potential issues associated with handling of the canisters throughout the process, including decontamination. Canister fabrication was initially included in the investigation but will be addressed in a separate study. Even though the proposed canister will be made from the same material as the current design, stress corrosion was a concern due to the reduced thickness and was addressed with environmental testing after establishing pertinent test conditions. The individual areas will be discussed separately.

2.0 Experimental Procedure

2.1 Thermal Modeling

Previous studies have been conducted to understand the temperatures in a standard canister during the pouring process[5]. A recent study[6] addressing nepheline formation used modeling to predict glass temperatures at various locations throughout the canister. Some of the criteria used for that study were also used in developing the Higher Capacity Canister (HCC) model. In addition, full scale canisters were instrumented to measure the glass temperature at various locations within the canister[7]. The actual data from this study was used to verify parameters for recent modeling. Since the thinner wall may allow for a faster heat transfer from the glass, it was necessary to have a better understanding of the thermal difference between the two types of canister. Thermal modeling was used in order to determine the differences in glass and surface temperature between the two wall thickness canisters. The COMSOL® model was used to predict the glass and wall temperatures at various heights during the fill and cool down stages. The inputs and results of the model are documented in a memo[8] and are discussed in Section 3. This information was used as input for another model used to predict potential stress differences introduced during the filling of the two types of canisters.

2.2 Stress Modeling

In order to supply input for additional testing, any differences in stress between the two canister types needed to be quantified. The goal was to determine the residual stress state of the canister after it cools. Using input from the thermal model[8] noted in the previous section, a finite element stress model was performed using ABAQUS® software. The 3:1 transition ratio from the top and bottom head to the thinner cylinder was kept the same in both models. After reaching a

maximum temperature on filling, the model assumed that the glass solidified at 930°F prior to cooling to room temperature. Since the area of the canister above the glass can contract more than the area in contact with glass, this creates a localized stress point. The transition from the thicker top head to the thinner wall was a particular area of concern. Four different levels of glass height were modeled. As seen in Figure 2-1, the different glass levels were: above the transition, at the top of the transition, at the bottom of the transition and below the transition. Material properties such as modulus of elasticity, yield strength, thermal expansion coefficients and density for 304L stainless steel were taken from ASME tables and are given in Calculation Number M-CLC-A-00466[9]. The description of the method used to model the structural response of the canister during glass pouring is also detailed in the document and the results are discussed in Section 3.

The mechanical loads for the canister are very small compared to the thermal stresses during the pour. The canister experiences hydrostatic pressure from the molten glass before it cools. After the glass solidifies, the hydrostatic pressure is removed. The force applied by the molten glass pool varies with depth as $\rho g \Delta z$, where ρ is the glass density, g is the acceleration due to gravity, and Δz is the downward distance from the surface of the glass pool. Preliminary analysis showed negligible impact from the mechanical loads of the canister so the hydrostatic pressure was conservatively applied at the beginning of the heat-up to the entire canister at once.

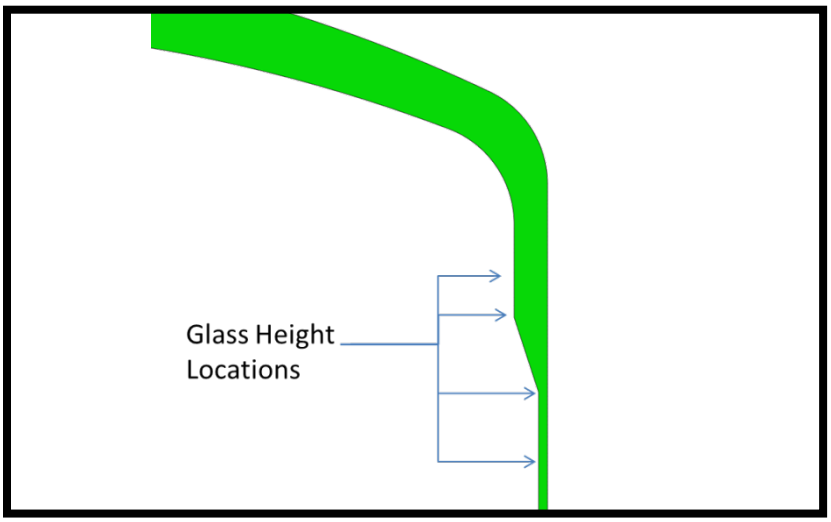

Figure 2-1. Glass Levels in Relation to Transition.

2.3 Canister Fabrication

The current canister must meet the criteria listed in the latest revision of the procurement specification[10]. Each vendor has procedures and test methods that are followed to guarantee an acceptable product will be manufactured. The use of a thinner material for the cylinder wall introduces several potential areas that must be addressed in the manufacturing method. These include changes to the welding procedures and possible addition of bands to minimize warping and provide additional support. Many vendors are reluctant to provide quotes without first manufacturing a prototype to better define the process changes necessary. After discussions with

Waste Solidification Engineering (WSE), it was decided that rather than requesting that vendors provide quotes to satisfy existing specifications, a different approach would be utilized. Energy Solutions was requested to develop a new drawing for the canister that included basic dimensions, without all the normal tolerances included on the current print. This drawing[11] would be presented to potential vendors who were asked to provide estimates of cost and achievable tolerances. When the Requests for Interest documents were returned, a decision could be made about the acceptability of the product.

2.4 Handling Calculations

The current DWPF canister was designed to meet a variety of physical requirements. The original minimum wall thickness[12] was specified as 0.335" and later changed to 0.340" based on multiple requirements[13]. Structural safety of the canisters was required in the Waste Acceptance Product Specifications (WAPS). The canisters are subjected to a variety of handling steps throughout the process in addition to the glass filling process. The general handling steps after delivery to DWPF, many of which are repeated, are listed below:

Removal from truck with forklift
Rotation to vertical position
Lifting/lowering by grapple hook with crane
Transfer with crane while held at nozzle with grapple
Through tunnels on transfer car
Rotation on turntables
Glass filling
Plug insertion
Frit blasting
Support while welding
Transfer to Glass Waste Storage Building (GWSB)

These handling steps of both empty and full canisters introduce a variety of stresses and loads on the canister. It was decided to evaluate several criteria that would be important during some or all of these situations rather than attempting to evaluate each individual step. The goal was to quantify the effects of the reduced thickness and identify any possible areas of concern with the thinner material. Bounding conditions would be determined and then calculations performed to compare the two designs. Areas evaluated include:

Compression Stress and Wall Buckling
Plug Insertion Demand
Handling Demand
Lifting
Dent Evaluation
Puncture Evaluation

The analysis of these conditions was conducted by the Structural Mechanics section of Savannah River Nuclear Solutions (SRNS) using closed form equations and finite element analysis (FEA) assessments. The results are documented in a Calculation T-CLC-S-00295[14], "Structural Evaluations of DWPF Canister at 0.13 Inch Wall Thickness" and are discussed in Section 3.0.

2.5 Decontamination

The decontamination step was treated as a separate case from handling due to the unique nature of the process. The water flows and pressures used to clean the canister are controlled to ensure decontamination while not causing damage to the canisters and minimizing the amount of material sent back for reprocessing. The operability of the decontamination system was verified and documented [15] prior to installation. While handling steps such at lifting and rotating turntables are involved in the decontamination process, the effect of the material removed during the frit blasting operation was used to determine the effect on the structural integrity of the canister.

2.6 Stress Corrosion

Material selection for the DWPF canisters was based on a variety of physical properties including strength and chemical durability. Corrosion resistance is important due to the potential exposure to environments that are conducive to corrosion in metals. The vapor space within the canister has been identified as the most likely area for corrosion attack. This is due to the possibility of water being present along with a concentration of condensed salts. Multiple studies of corrosion,[16] salt concentration,[17,18,19] dew point,[20,21,22] temperature,[23,24,25] have been conducted with the overall consensus that stress corrosion is the most likely form to cause a threat to the integrity of the canister. Short term environmental testing with defined conditions was chosen as the best method to evaluate the differences between the canisters. The modeling conducted earlier in this study was used to help define the stress parameters for the testing. Small scale canisters were manufactured and filled with glass in order to introduce stress. In addition, U-bend samples were incorporated to include stress values beyond those deemed possible in the canister design. Measurements were taken to determine the strain produced and then the samples were subjected to environmental testing for 3 months. The testing was documented and the results[26] are discussed in Section 3.6.

2.7 Quality Assurance

Requirements for performing reviews of technical reports and the extent of the review are established in manual E7 2.60. SRNL documents the extent and type or review using the SRNL Technical Report Design Checklist contained in WSRC-IM-2002-00011, Rev.2.

3.0 Results and Discussion

3.1 Thermal Modeling

The results of the thermal modeling at different canister heights are shown in Figure 3-1 through Figure 3-4. Once the glass reaches the height indicated in the graphs, the peak temperature difference in the surface of the canister is between 60 and 80°F. The graphs also show that the thinner walled canister increases and decreases temperature at a slightly faster rate than the original. When comparing the internal and outer surface temperatures for both sets of canisters, the thinned walled canister has a 3°F ΔT as compared to a 5°ΔT for the original design. The small temperature difference on cool down is not expected to have a measurable effect on crystal formation in the glass.

One potential area of concern had been the infrared camera used to monitor the glass height during pouring. A large temperature difference could affect the accuracy or integrity of the camera. Given the distance between the camera and canister, coupled with the small differences in surface temperatures; the HCC would pose no threat.

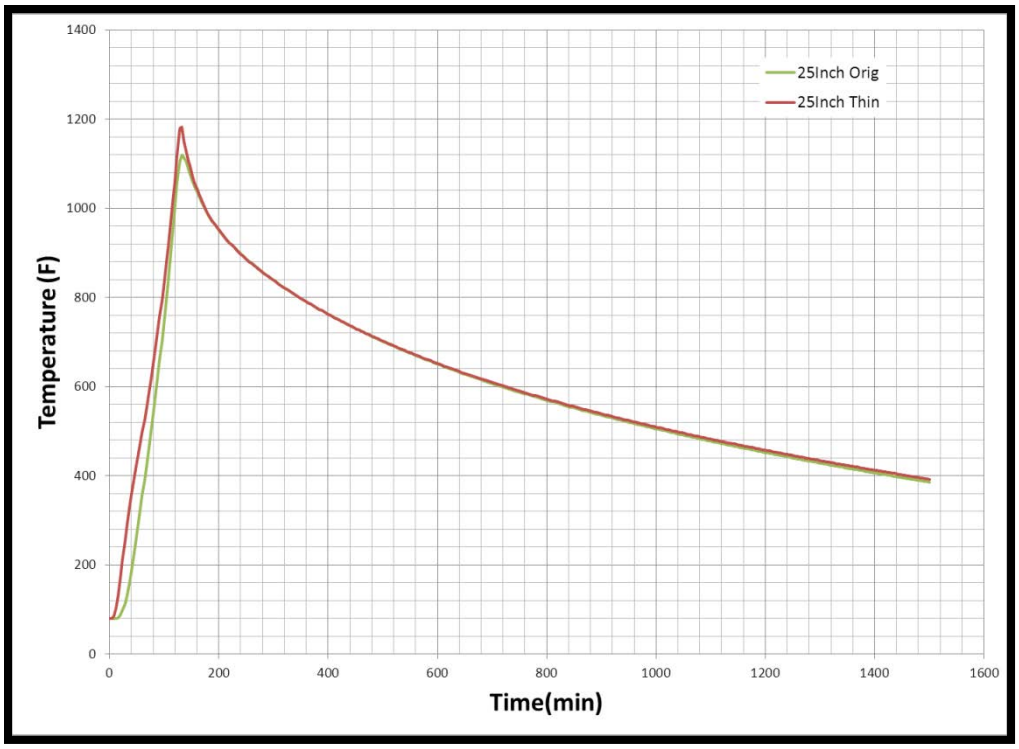

Figure 3-1. Predicted Canister Temperature Profile at 25 Inches from Bottom

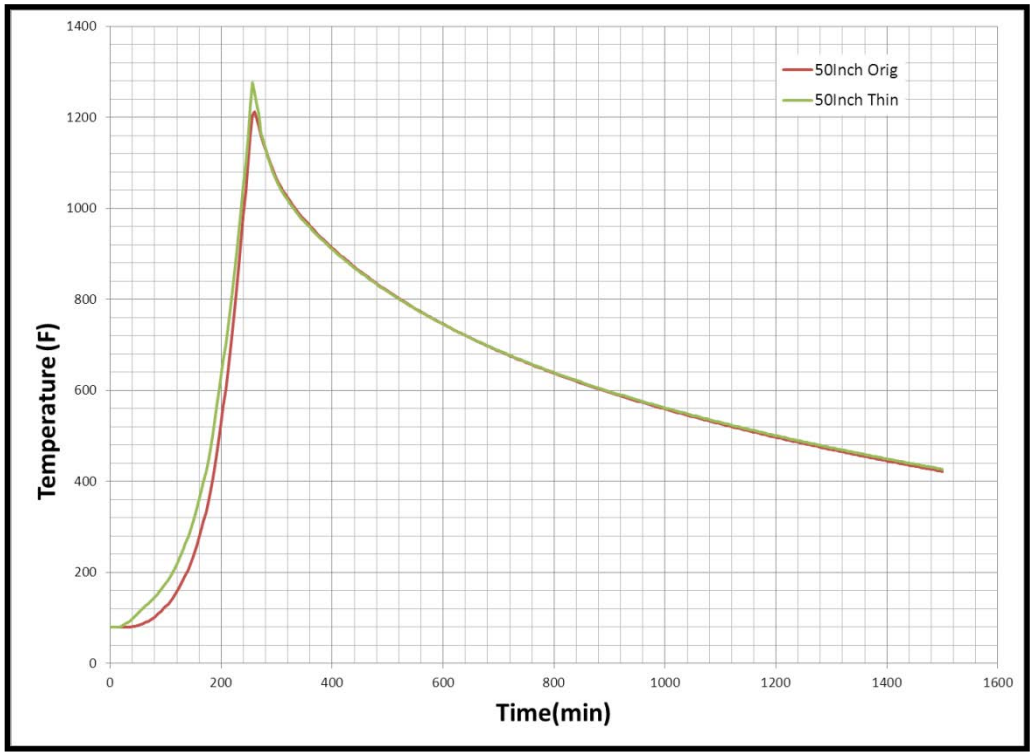

Figure 3-2. Predicted Canister Temperature Profile at 50 Inches from Bottom

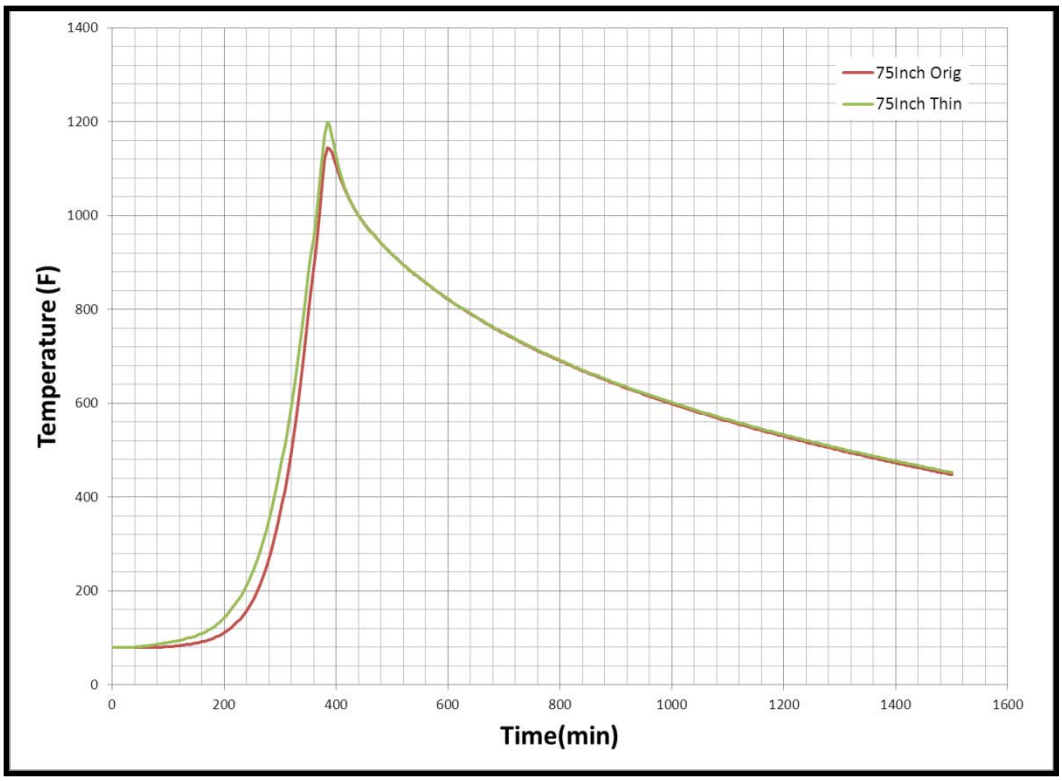

Figure 3-3. Predicted Canister Temperature Profile at 75 Inches from Bottom

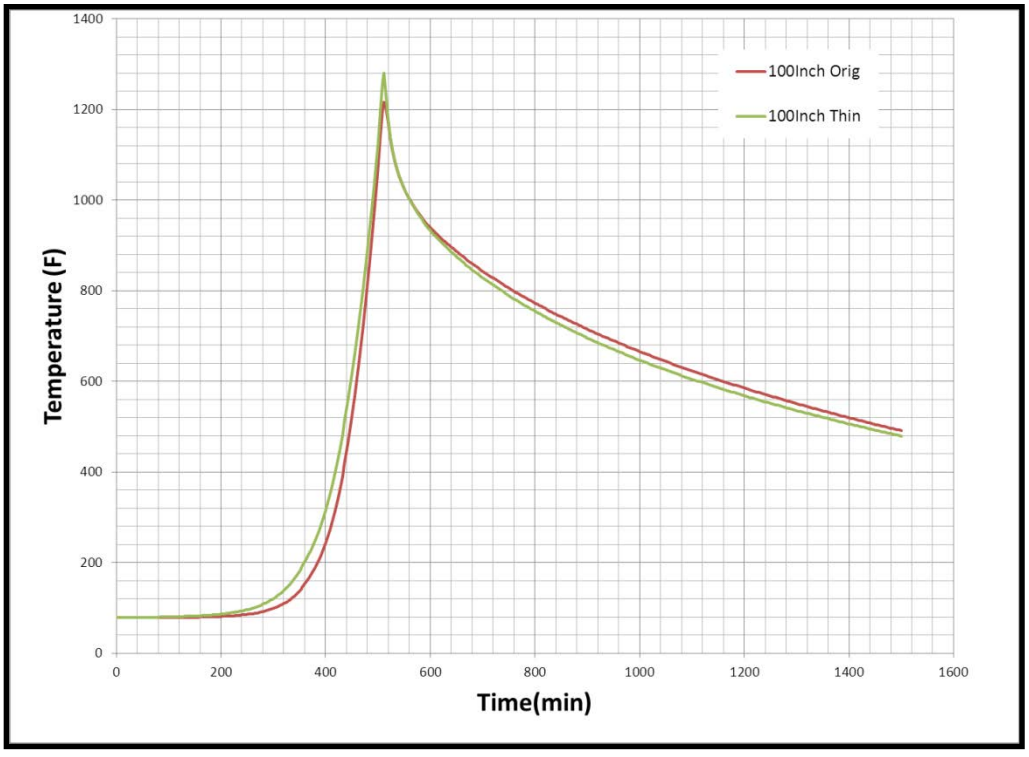

Figure 3-4. Predicted Canister Temperature Profile at 100 Inches from Bottom

It was noted that the results of the simulations from this study yielded higher temperatures than found in the experimental data, which should yield a conservative basis for the stress analysis. The higher pour rate used for this study (400 vs. ~230 lb/hr) could also contribute to the elevated temperatures.

3.2 Stress Modeling

The level of the glass in the canister is important since the portion of the canister against the glass cannot contract, while the portion above the glass transition is free to move. This creates a localized stress point which can lead to higher deformation. The thin-to-thick transition along the canister wall was identified as a potential area for increased stress and strains. The model was run for each canister type based on the relation of the glass height to the transition as discussed in Section 2.2.

Based on the temperature change seen by the canister, enough stress is produced to cause the canister to go beyond the yield point (approximately 0.02% strain). It was therefore more appropriate to discuss the results in terms of strains since the subsequent physical testing will place a strain on the canister specimen before environmental exposure. If the canister were uniform and the glass transition were ignored, the strain could be approximated from the linear coefficient of thermal expansion times the change in temperature.

The bottom of the canister is identical for the two designs. The peak strain at any location occurs at a transition along the base of the canister. This strain is likely artificially high since the straight to curved transition in the model does not match the smooth transition in the physical canister. The peak strain in this location is 3.3%, see Figure 3-5. This is a low strain and isn't in a critical region for long term storage of the canister. The strain at this location is the same for both designs.

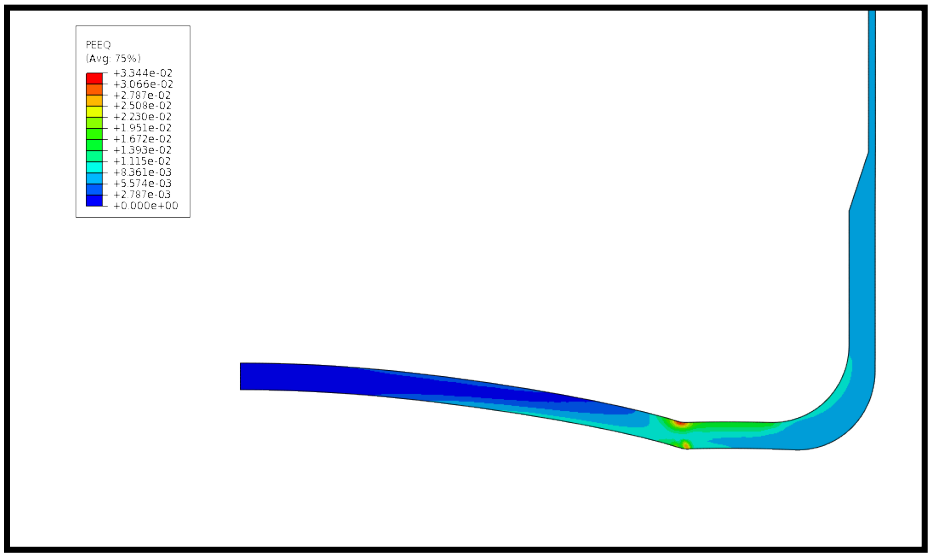

Figure 3-5. Max PEEQ for Thin Canister.

The models with the height above the thin-to-thick transition produced similar results between the two canister designs. The strain is localized to the hard transition point. The strains for the thin and thicker design are 2.9% and 3.1%, respectively. This is shown in Figure 3-6 and Figure 3-7.

Outside the localized transition region, the strains in the wall are approximately 0.8% for both designs.

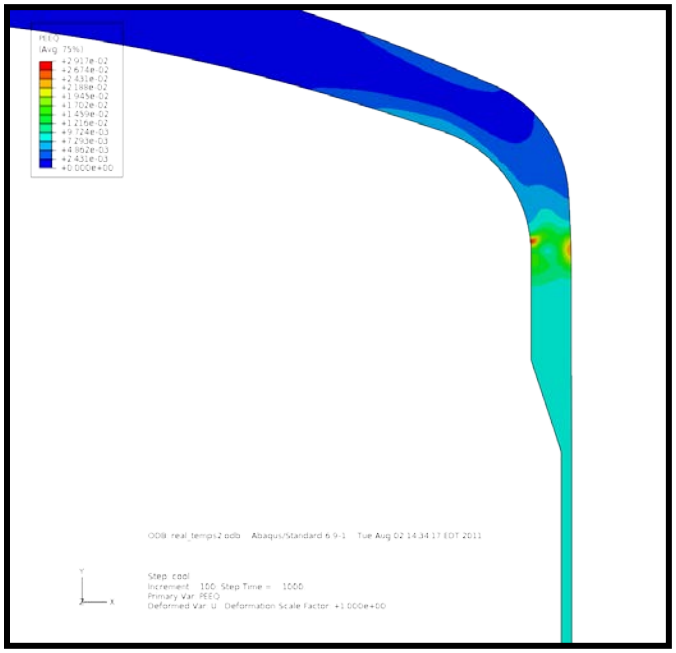

Figure 3-6. PEEQ above the Thin-to-Thick Transition for the HCC Canister.

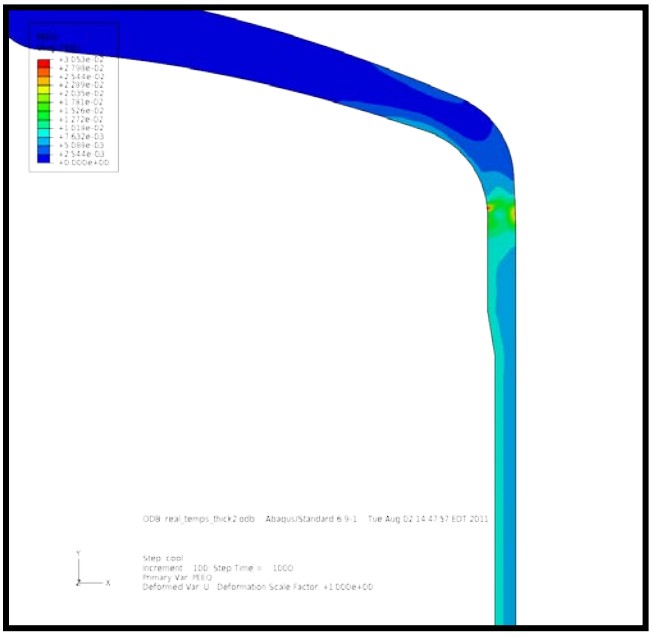

Figure 3-7. PEEQ above the Thin-to-Thick Transition for the Standard Canister.

For models with the transition around the thin-to-thick transition, the thinner design sees more strain than the thicker design. This is due to the bending above the transition caused as the

canister tries to contract to its original shape. With glass at the top of the transition, the strains for the HCC and standard designs are 2.5% and 1.9% respectively as shown in Figure 3-8 and Figure 3-9.

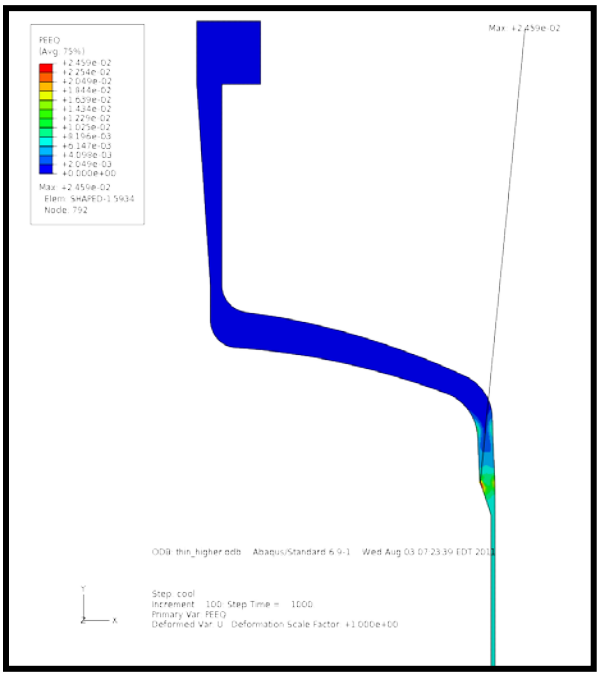

Figure 3-8. PEEQ at the Top of the Thin-to-Thick Transition for the HCC Canister.

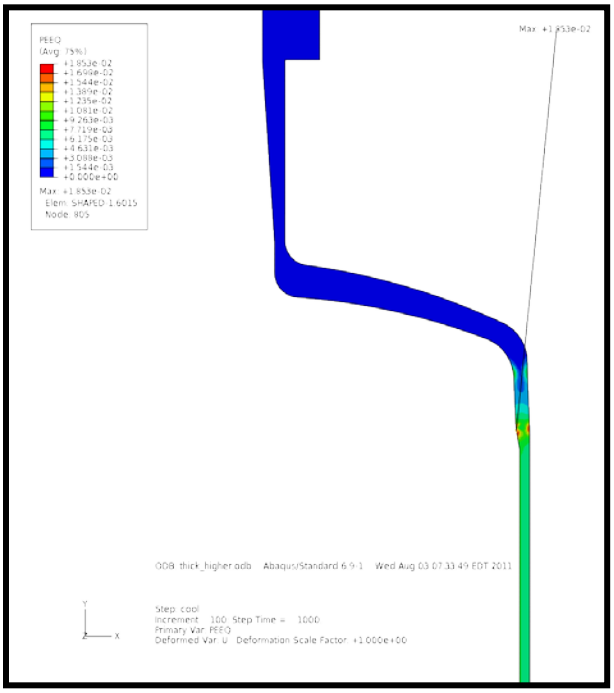

Figure 3-9. PEEQ at the Top of the Thin-to-Thick Transition for the Standard Canister.

With the glass at the bottom of the thin-to-thick transition, the results are similar. The strain in the HCC design is 2.8% while the standard design is 1.9% as shown in Figure 3-10 and Figure 3-11.

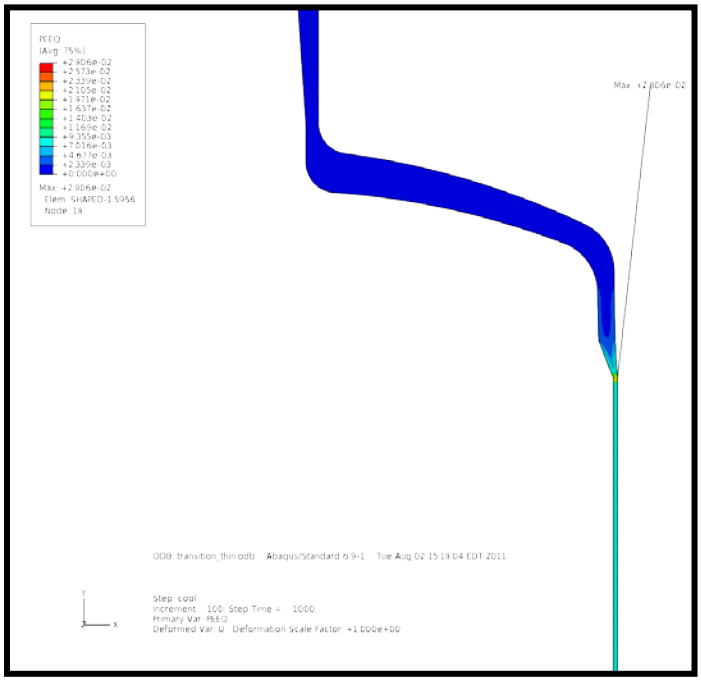

Figure 3-10. PEEQ at the Bottom of the Thin-to-Thick Transition for the HCC Canister.

Figure 3-11. PEEQ at the Bottom of the Thin-to-Thick Transition for the Standard Canister.

With the glass below the thin-to-thick transition in the canister, the results follow the same pattern. The strains are 2.9% for the HCC and 2.0% for the standard design - see Figure 3-12 and Figure 3-13.

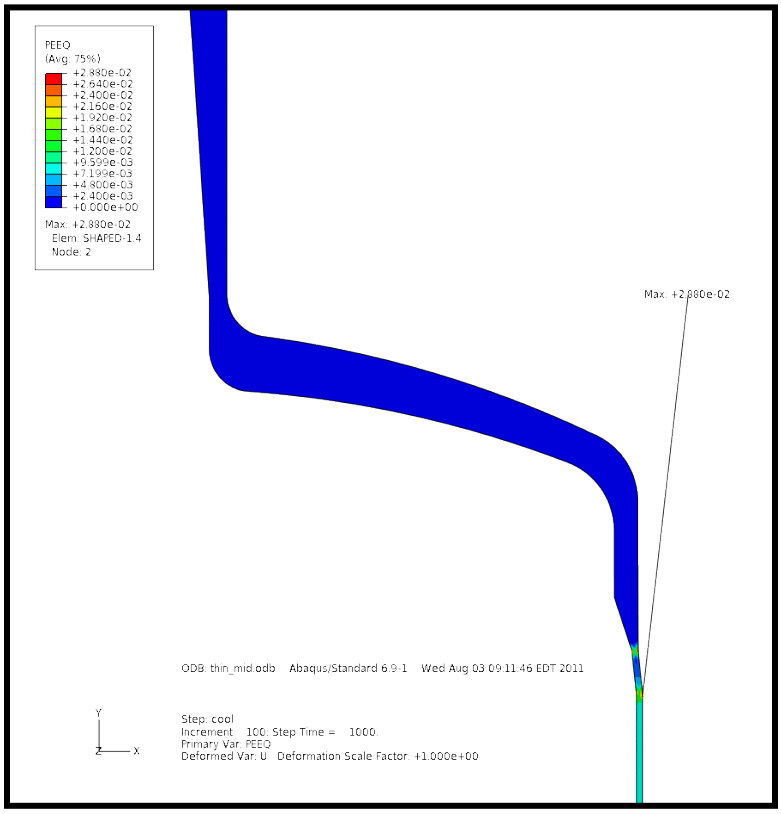

Figure 3-12. PEEQ below the Thin-to-Thick Transition for the HCC Canister.

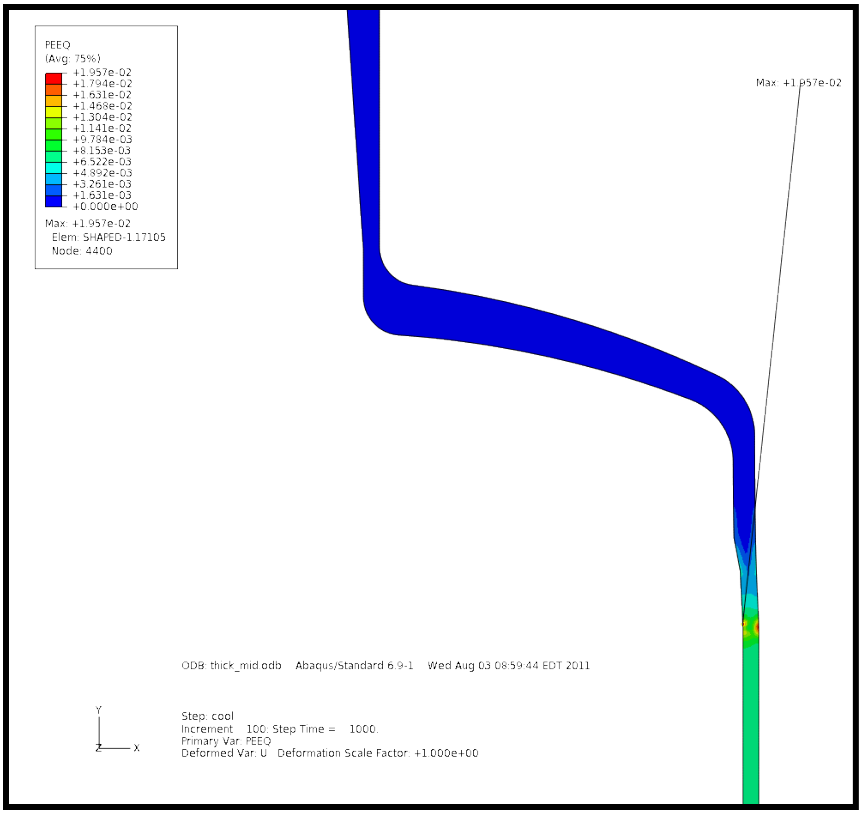

Figure 3-13. PEEQ below the Thin-to-Thick Transition for the Standard Canister.

3.3 Canister Fabrication

Eight vendors were contacted by Energy Solutions for interest in manufacturing the HCC design. Six suppliers returned estimates for manufacturing 2 model prototypes along with cost and schedule estimates to produce a large production run (275 canisters). Additionally, some vendors submitted comments regarding proposed modifications or potential manufacturing techniques to provide a higher degree of confidence in meeting the requirements.

3.4 Handling Calculations

As discussed in the experimental procedure section, calculations were performed to estimate the differences between the two designs during a variety of conditions. The details of the study are found in the document[14] referenced in Section 2.4, but highlights are included below.

3.4.1 *Compression and Wall Buckling*

Calculations for both canister types indicate that the critical buckling stress of the wall section is in the plastic stress regime for either design. Conservative compressive load limits for the canister wall were computed based on the material yield strength at the load condition temperature. This included the pour condition, where a small compressive load from the bellows is in effect and small regions of the canister wall can see 1300 ºF. The results of the calculations are given in Table 3-1. For either canister wall thickness, the compressive load limits are still dictated by the allowable load on the upper shoulder region of the canister.

Table 3-1. Compressive Load Limits of Canister Types

Property	Units	Standard Canister	HCC
Wall Compression Limit at 1300ºF	Pounds	339,000	118,000
Wall Compression ASME Code Allowable at 1300ºF	Pounds	111,600	35,300
Wall Compression ASME Code Allowable During Handling Conditions	Pounds	167,000	49,000
Canister Load Limit Based on Top Head Shoulder Region	Pounds	14,500	14,500

3.4.2 *Plug Insertion Demand*

The force of the plug insertion is nominally 80,000 lbs. The machine limit is 150,000 lbs. During the insertion process, the canister is supported beneath the top flange. Therefore the load path is from the ram through the canister top flange and then directly into the bottom electrode support platen. The load path is identical to the electrical current path shown in Figure 3-14. The canister body is not in the load path.

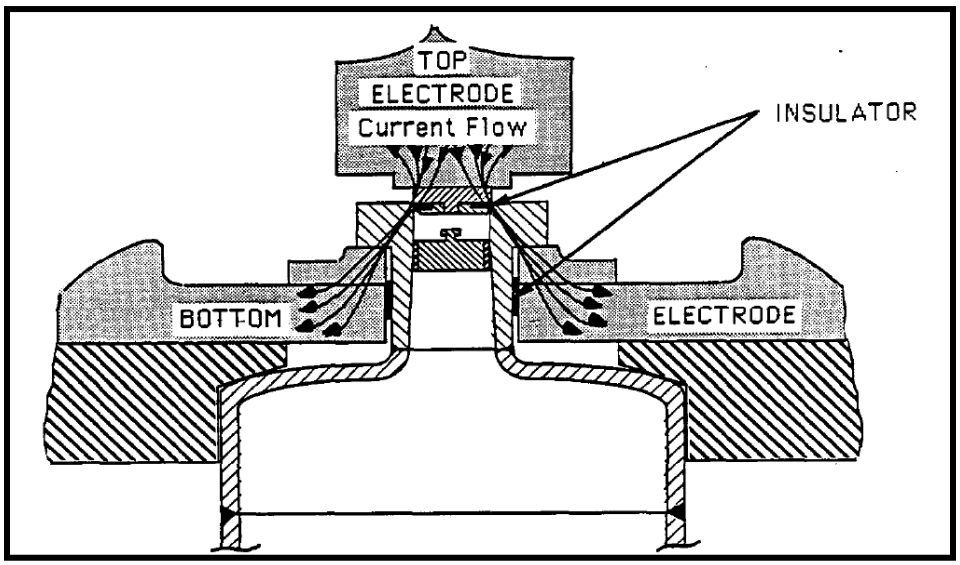

Figure 3-14. Load Path and Electrical Current Path During Plug Weld.

3.4.3 *Handling Demand*

Shipping and transport of empty canister will result is less than 5G vibration and impact loads. For the 1100 lb container, this results in a maximum of 5500 lbs demand vs. a

capacity (at handling temperatures) of 49,000 lbs for the HCC and 167,000 lbs for the current design.

3.4.4 *Lifting Demand*

Estimated weight for the current canister is 1100 lbs empty and 5500 lbs when full. The HCC has reduced metal weight but has a gain in glass volume. Since glass is less dense than metal, there will be a reduction in the filled weight. The analysis uses the same 5500 lbs for both cases to provide a conservative basis. The dynamic stress levels calculated during a canister lift are 194 psi for the current design and 561 psi for the HCC. These stresses are well within a yield/3 criteria of 5,200 psi (using 600º F as a bounding condition for the lift). As for the compressive load conditions, the lift condition is limited by the canister top head shoulder region for either the current or HCC design.

3.4.5 *Dent Evaluation*

The empty canisters are shipped in horizontal orientations. Several lift points and worst case conditions were considered. Using a horizontal canister being supported only from the top in a cantilevered fashion is a worst case configuration not used in DWPF. Even under this extreme condition, the calculated stress of 5519 psi is less than the allowable ASME limit of 9500 psi.

The units are delivered in racks of 9 canisters with a limited number of supports. Using a single lift point provides a conservative calculation basis for a variety of possible support configurations. A 3-D model of the canister using ABAQUS fully integrated shell elements was created. A 4 inch wide flat strip was modeled and placed at the mid-height of the canister. This rigid strip bounds any contacting interface (fork lift blade, cradle, etc.). The denting occurs as the canister is pushed in to the support until the reaction force equals twice the canister weight. An image of the model under load is shown in Figure 3-15. Note: Deflection total on graph includes 0.002” initial gap between contact surface and canister wall.

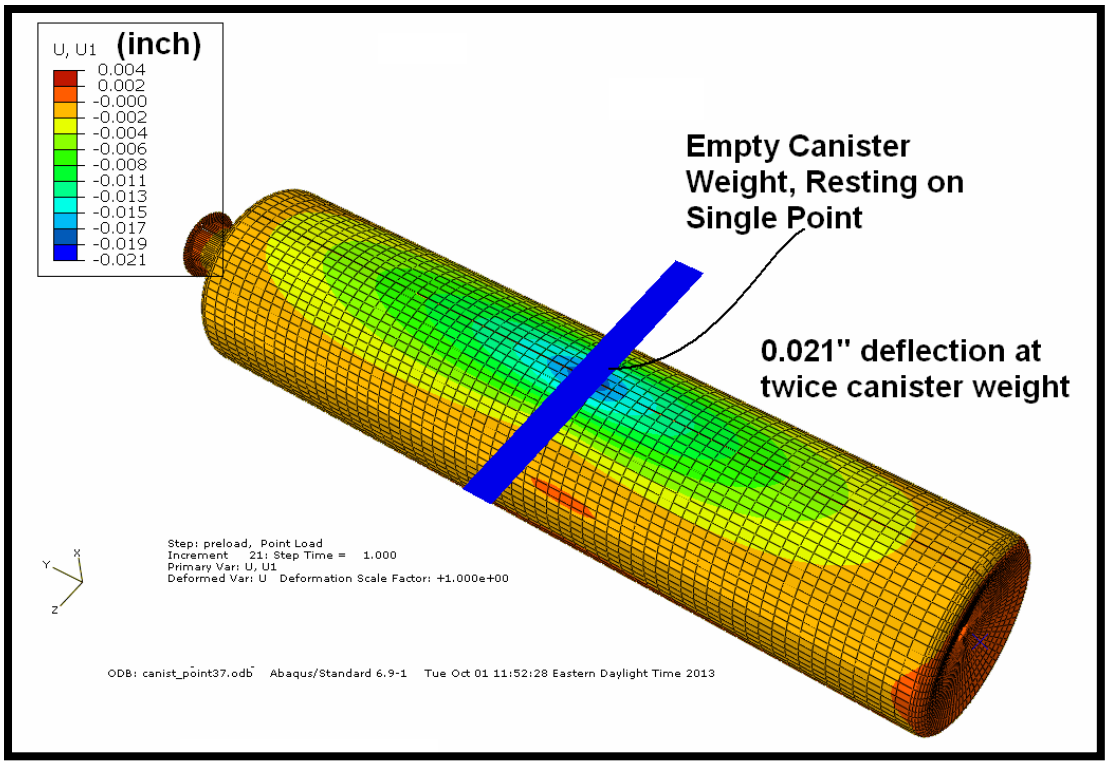

Figure 3-15. Canister Deflections for 2X Self-Weight Load Acting at a Single Point, Canister Wall Thickness = 3/8 inch. Results Show 0.018 inch Deflection.

The stresses resulting from the load being placed on the canister are shown in Figure 3-16. This shows that even under maximum stress condition, the region of contact is still less than yield stress.

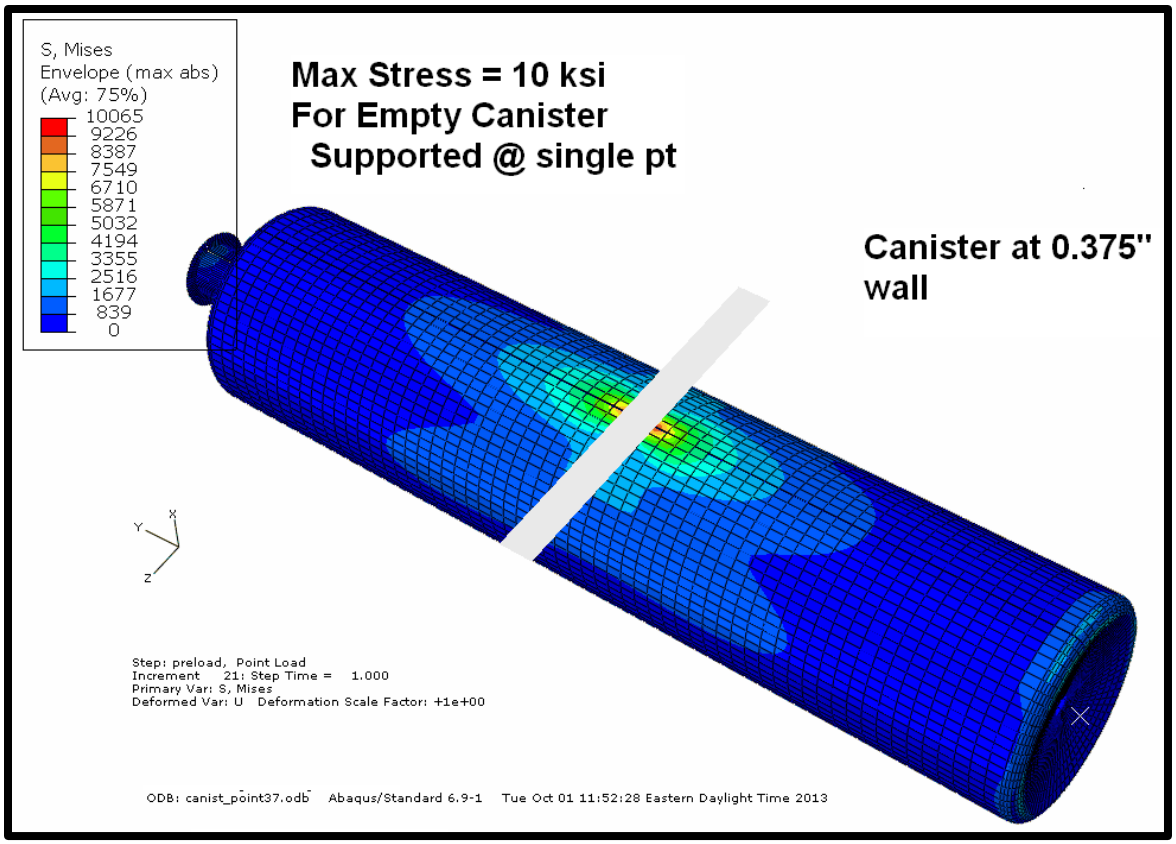

Figure 3-16. Canister Stress For 2X Self-Weight Load Acting at a Single Point, Canister Wall Thickness = 3/8 inch. Results Show 10 ksi Maximum Stress, Less than yield.

The load-deflection history is shown in Figure 3-17. The linearity of the plot shows no instability or permanent dent under load.

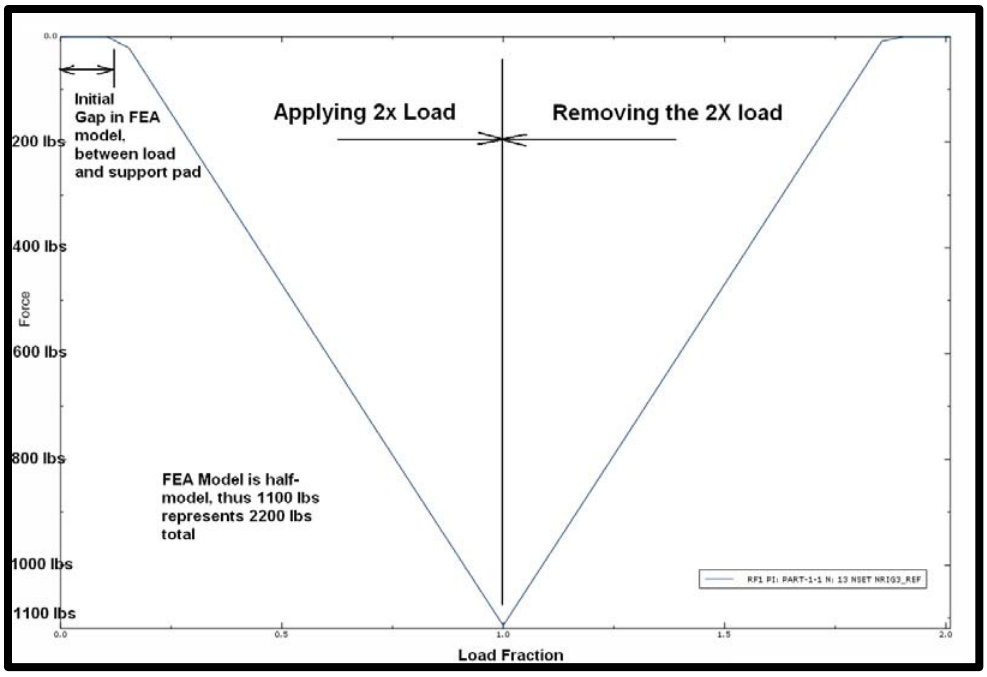

Figure 3-17. Load-Deflection History of Canister Wide Wall for 2X Self-Weight Load Acting at a Single Point, Canister Wall Thickness = 3/8 inch. Results Show Pure Elastic Behavior and No Permanent Deflection.

The model was repeated using the HCC design and yielded similar results up to a 1X load. As the load was increased to 2X, the HCC began to show more deflection and higher stresses. The maximum stress conditions before and after load removal are shown in Figure 3-18 and Figure 3-19.

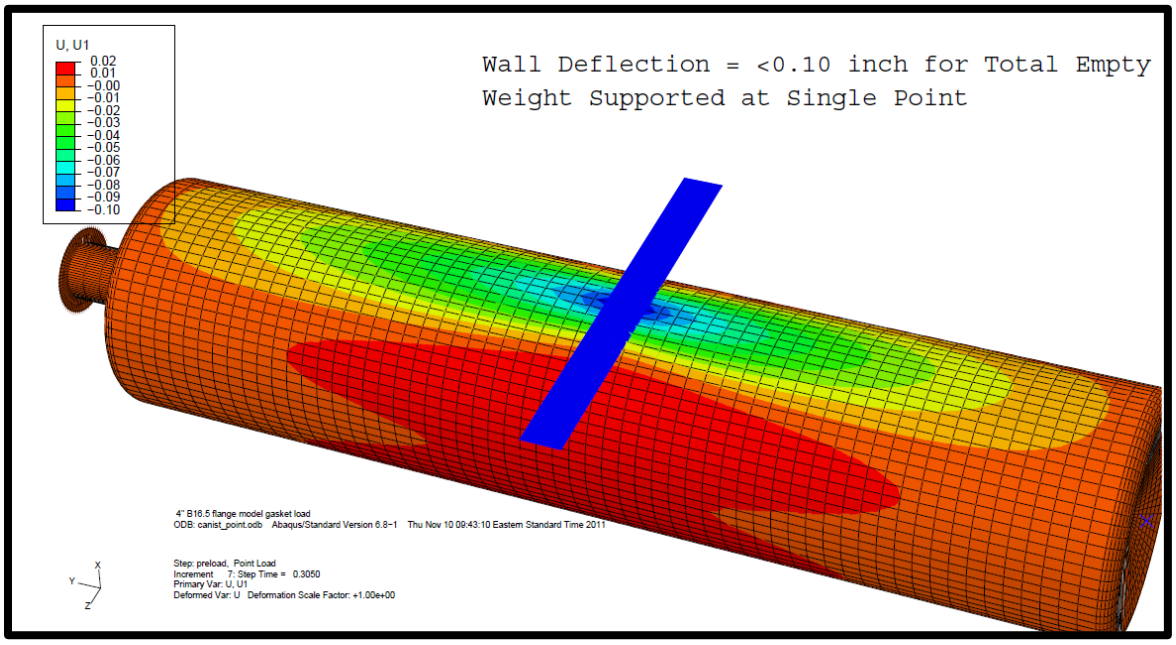

Figure 3-18. Canister Deflections For 2X Self-Weight Load Acting at a Single Point, Canister Wall Thickness = 0.13 inch. Results Show 0.10 inch Deflection.

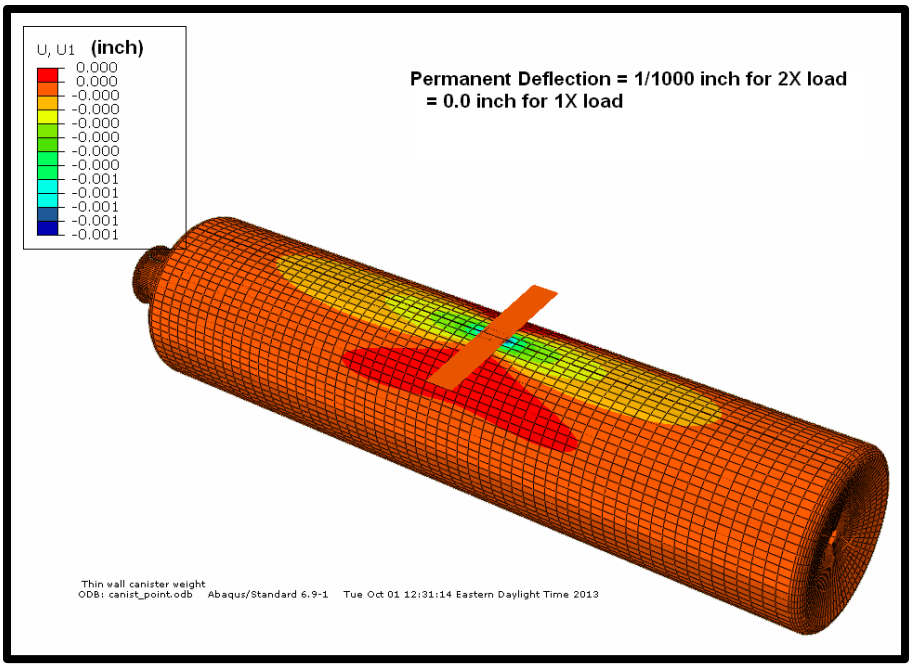

Figure 3-19. Canister Deflections After Removal of 2X Self-Weight Load Acting at a Single Point, Canister Wall Thickness = 0.13 inch. Results Show 1/1000 inch Permanent Deflection.

The HCC results indicate some yielding at 2X conditions with 0.1 inch deflection at 2X load. The permanent deformation after load removal is essentially zero. A combined load deflection history is shown in Figure 3-20.

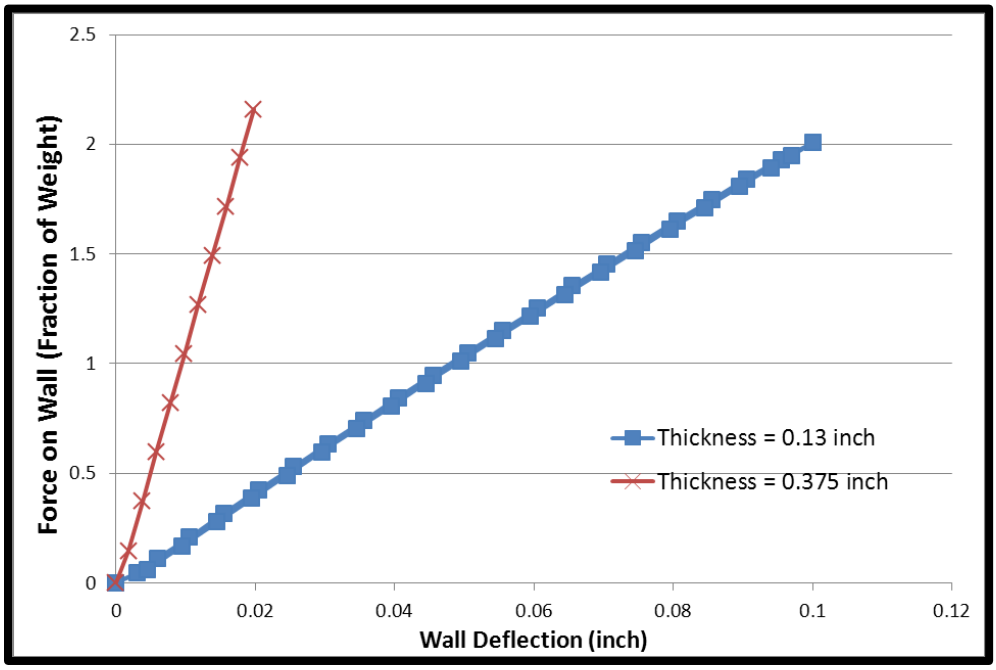

Figure 3-20. Load-Deflection History of Canister Wide Wall for 2X Self-Weight Load Acting at a Single Point,

The dent resistance of a cylindrical wall is related to the bending stiffness which is proportional to thickness cubed. Load conditions during handling are related to weight which has a linear variance with wall thickness. The resultant self-weight resistance to denting will be dependent on thickness squared. The predicted dent resistance ratio would be $0.375^2/0.13^2 = 8.23$. The deflection values in the FEA solution graphed in Figure 3-20 show that the relative deformation resistance (0.10"/ 0.018" = 5.6) is similar to the relative theoretical predictions.

3.4.6 *Fork Lift Clamping*

In addition to being stored on racks, the canisters are moved several times using a fork lift with a clamping device. The clamps are curved to match the radius of the canister and have pads on the clamping surface. The clamping force is limited to a maximum of 5053 pounds. The forces on each canister type were modeled with the combination of clamping force and canister weight. The stresses introduced in the standard canister wall allow more than a 3X safety factor against yielding. Figure 3-21 shows the maximum deflection in the wall of the standard canister during clamping by the fork lift. When the clamping force is removed, there is no permanent deflection.

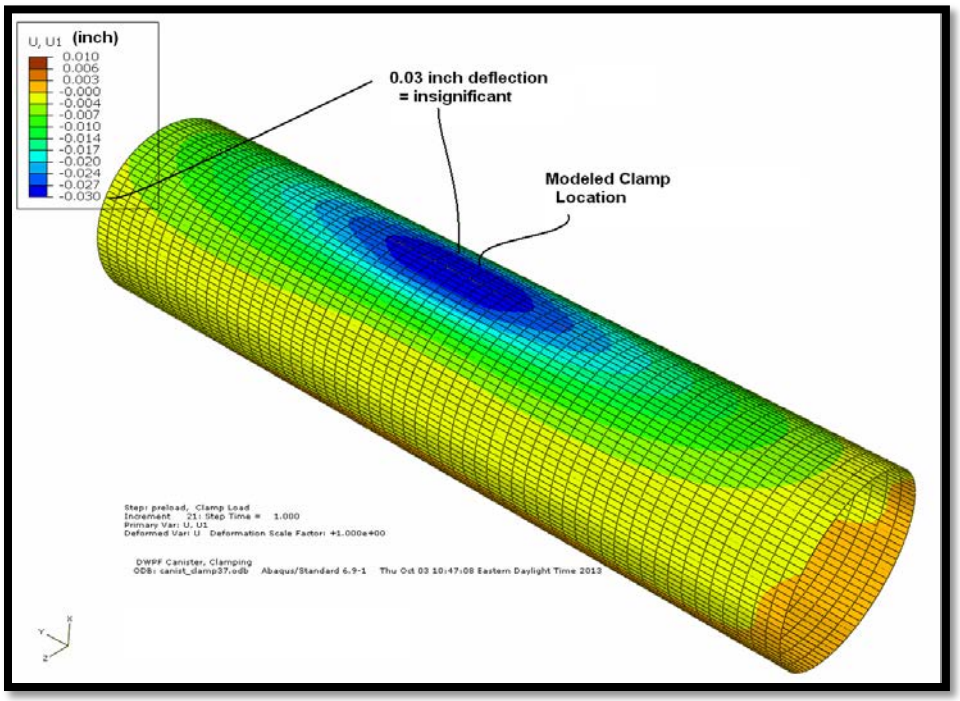

Figure 3-21. Canister Deflection for Worst Case Handling Clamp Load (6300 lbs) for Standard Canister.

When the HCC canister was modeled, the stresses approached the yield strength in localized regions. The wall deflection was ¼" under the clamp load conditions. When the clamp pads were included in the model, the high stress points were reduced to only the clamp corners, which are of no structural consequence. Figure 3-22 shows the permanent deflection after clamp removal was 0.002", which is also of no structural consequence and not detectable.

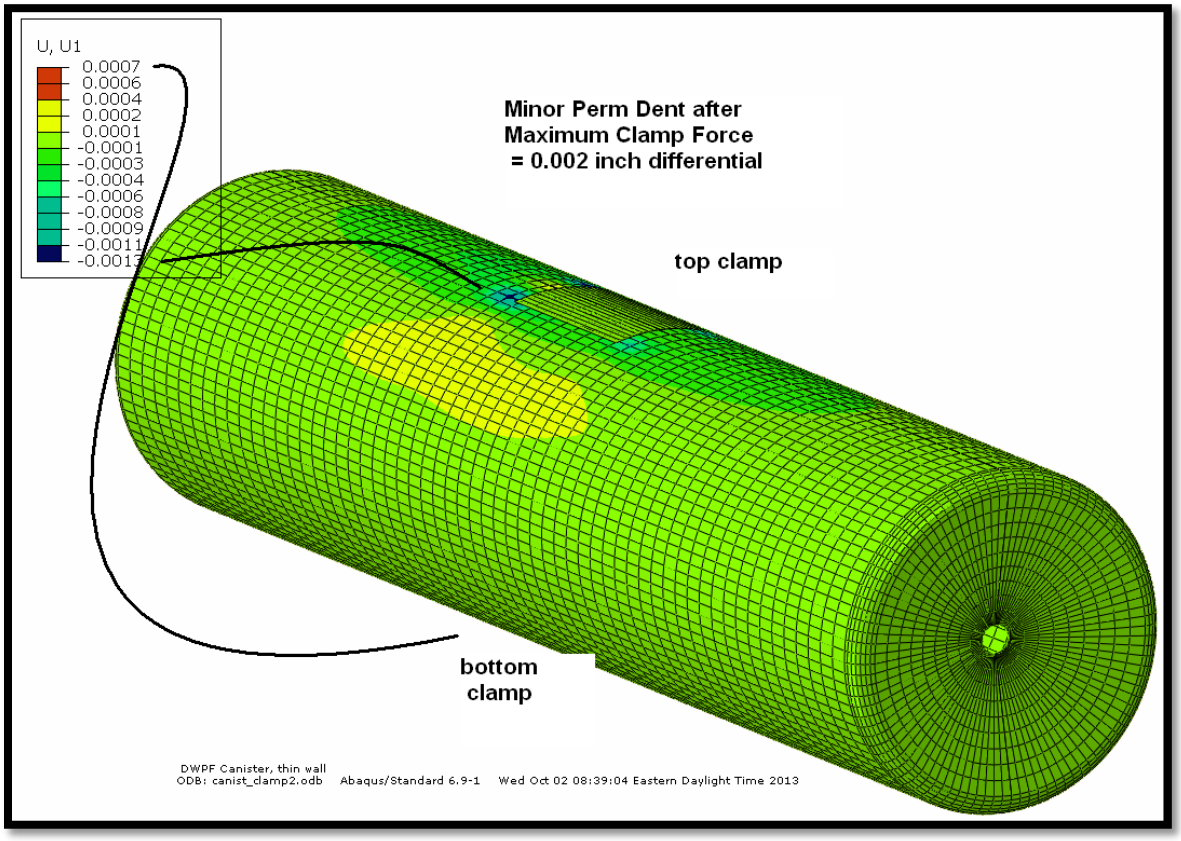

Figure 3-22. Canister Deflection after Removal Deflection for Worst Case Handling Clamp Load (5700 lbs) for HCC Canister.

3.4.7 *Puncture Resistance*

It is likely that an empty canister would either deform or push away from a force large enough to puncture the wall. This would probably be even more likely in the case of the thinner walled canister. The puncture resistance of both empty canister designs was calculated using a standard formula developed by Ballistic Research Laboratories shown below:

$$\text{Perforation Resistance} = \propto (672 * D_1 * t_{p1})^{3/2}$$

where D_1 is the effective projectile diameter and t_{p1} is the thickness.

This shows that the resistance is proportional to thickness to the 1.5 power. Using the current and HCC designs ($0.375^{1.5}/0.13^{1.5}$) yields a factor of 4.9.

3.5 Decontamination

Decontamination of the canisters is accomplished through frit blasting. Early testing[27] indicated that a canister could be decontaminated with a weight loss of less than 5 mg/in^2. Additional testing[13] documented that using the current process conditions yielded a total removal of ~ 70 grams from the surface of each canister or approximately 10 mg/in^2. This amount corresponds to an average removal depth of 0.001 inch. Calculations for the HCC thickness were performed using a rounded down value of 0.13 inch. This thickness bounds the nominal thickness, even accounting for the potential for 0.001 inch loss in thickness due to decontamination. The calculation involved several load conditions and the behaviors with the highest dependence on thickness were proportional to the thickness squared. The largest effect of the 0.001 inch wall thickness loss would be on perforation resistance as shown below.

$$\text{Perforation resistance} = 0.1345^2/0.1335^2 = \text{factor of } 1.015 \text{ or a } 1.5\% \text{ change}$$

3.6 Stress Corrosion Cracking

Dimensional measurements on the canisters indicate that both longitudinal and hoop tensile strains/stress are created in the canister wall during cool down. The calculated hoop stress for the filled canister is 40-50 KSI. Calculated longitudinal stress ranged from 11 KSI to 22 KSI. Material certification data for the 304L welded pipe includes a value of 38.7 KSI for yield stress and 92 KSI for ultimate strength. The maximum hoop stresses in the sample canister walls are higher than the 304L material yield strength which was also predicted by the stress modeling.

An accelerated (3-month) aging study of several samples fabricated to simulate potential of stress corrosion cracking for the HCC design was conducted. Selected conditions were 30% relative humidity, 60°C temperature, 5000 ppm chloride and 500 ppm sulfate concentration. Samples of a recent Melter Feed Tank (MFT) process batch were reviewed[28] to verify that the current process salt concentration were not dramatically different from those experienced in earlier corrosion studies.

Small scale canisters were fabricated to provide a test sample with stress properties similar to the DWPF canisters. A transition from thicker to thinner material was included in the test canister design. Certified 304L pipe was used to ensure direct comparison to the DWPF canister material. In addition to the canisters, U-bend (ASTM G30-97) samples were also sampled to provide a wide range of stress conditions for evaluation. A sample canister with measured height locations and U-bend coupons are shown in Figure 3-23.

Figure 3-23. Sample Canister and U-bend Coupons

The small scale canisters were filled with DWPF type glass to simulate the stress incurred during the pouring operation. Three 600 ml platinum crucibles containing DWPF type glass were heated to 1200°C for 1 hour prior to being poured into the test canister. Approximately 2 minutes were required to fill each canister. Dimensional measurements at multiple locations made before and after glass pouring gave actual stress values.

A mixture of salt solution was sprayed onto the samples and then dried to deposit the salt directly on the surface of the stressed material. This process was repeated until a layer of salt was deposited prior to placing the samples in the environmental chamber. Temperature and humidity were monitored throughout the test period. Periodic adjustments were made to maintain the humidity at the target of 30%. Analysis of the data shows that the average relative humidity and temperature were 31% and 60°C, respectively.

The canisters and U-bend coupons were removed after 3 months in the environmental chamber. Condition of the canisters and U-bend coupons after exposure is shown in Figure 3-24 and Figure 3-25.

Figure 3-24. Scale Canisters after Exposure to Environmental Chamber for 3 Months.

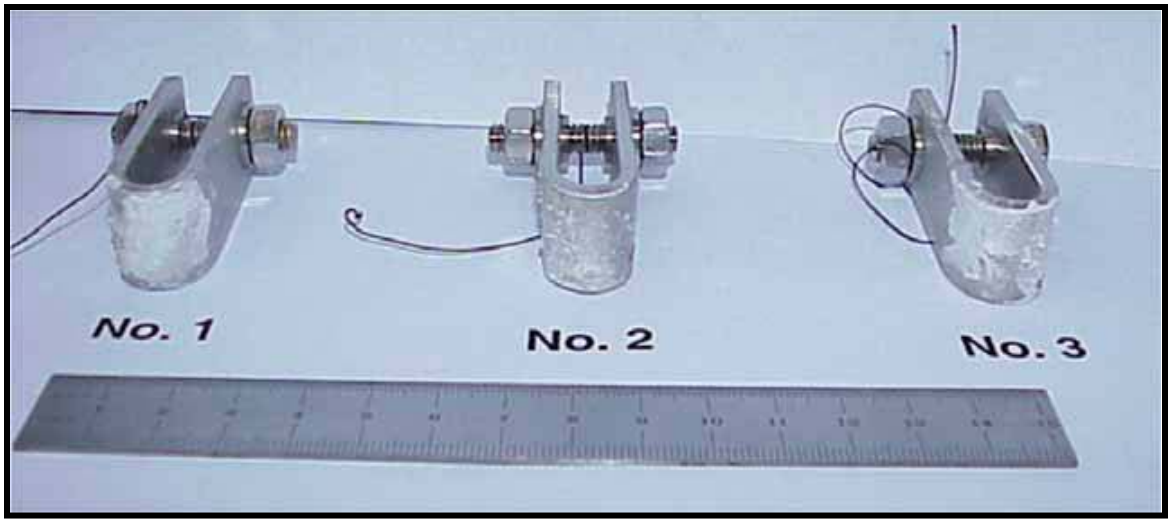

Figure 3-25. U-bend Coupons after Exposure to Environmental Chamber for 3 Months.

The samples were cleaned prior to the application of a dye penetrant and then examined for cracks. No evidence of crack-like indications was found on the U-bends or canister surfaces; including along the longitudinal seam weld. One U-bend coupon had an indication along the low stress section of the "U" that appears to be a result of the production method. This is shown in Figure 3-26 which also demonstrates the absence of cracking in any of the stressed region.

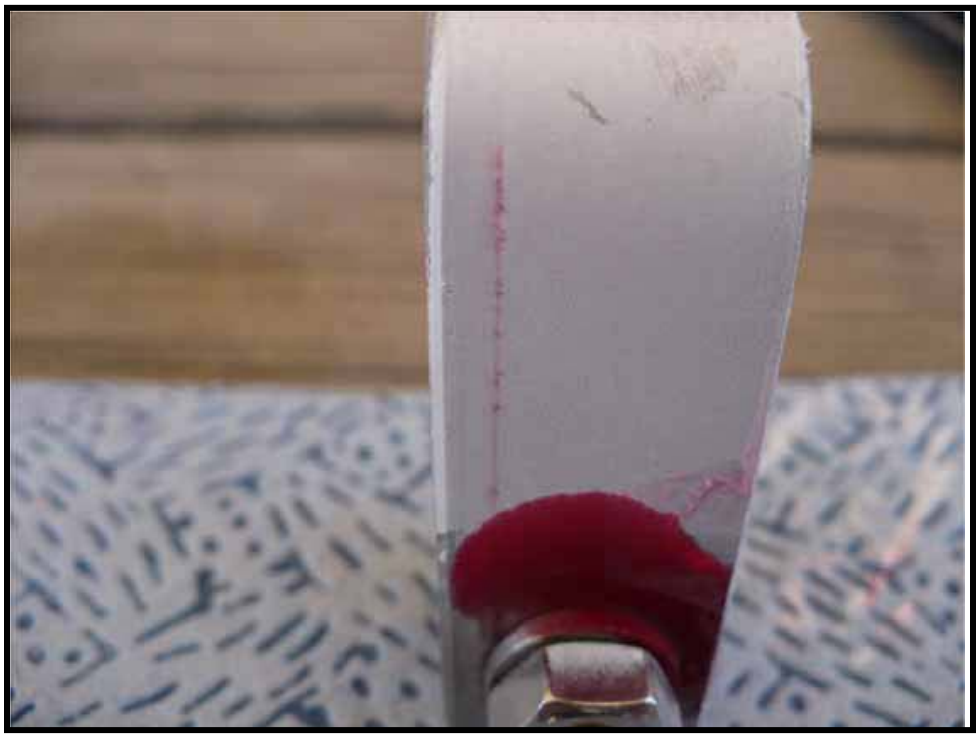

Figure 3-26. U-bend Coupon Showing Formation Artifact.

The complete details of the environmental testing and results are addressed in a separate memo[26] as discussed in Section 2.6.

4.0 Conclusions

4.1 Thermal Modeling

The model showed a maximum difference between the two canisters surfaces of between 60° and 80°F. The model also indicated that the thinner walled canister increases and decreases temperature at a slightly faster rate than the original. When comparing the internal and outer surface temperatures for both sets of canisters, the thinned walled canister has a 3°F ΔT as compared to a 5°F ΔT for the original design.

4.2 Stress Modeling

Stresses developed from metal contraction as the canister cools are essentially the same when comparing the standard canister and the HCC. Thermal stresses arise from differential expansion between the canister wall and the glass contents, and also from through-wall thermal gradients during the initial pouring. The predominant strain/strain was due to the differential between the glass and the steel wall. As the thermal expansion of the metal wall expands at a larger rate than the glass, the reverse occurs with cooling, and the metal contracts against solidified glass. This produces secondary localized stress in both the standard and HCC and of the same magnitude in each (Ref. T-CLC-S-00295). The result is an insignificant dimensional and strength change (mainly strain hardening of the material) for both the standard and HCC. Stresses in the HCC due to through-wall temperature gradients during glass pouring would tend to be less than those occurring currently in the standard wall canister.

4.3 Canister Fabrication

As stated previously, canister vendors were asked to supply information and quotes on manufacturing the HCC. Dimensional tolerances may have to be revised to allow for changes in the manufacturing process. The models developed in this study used existing dimensional tolerances. Transition ratios from thicker end components to the uniform wall thickness section were kept the same. If the selected manufacturing techniques result in different transitions or other structural changes, they would need to be addressed. This investigation reviewed the finished product with two different thicknesses without addressing the fabrication.

4.4 Handling

The handling portion of the evaluation covered a range of operations performed on the canister. The specific areas of concern will be addressed separately.

4.4.1 *Compressive and Wall Buckling*

The compressive load carrying ability of both canisters is governed by stress rather than geometric buckling. The relative compressive strength is linear related to the wall thickness for a factor of 3.750/0.13 = 2.9. The top head limits compressive loads to 14,500 pounds so in either case, the wall thickness is not limiting.

4.4.2 *Plug Insertion*

The top head component of both canister designs is the same. The method of support during plug insertion does not load the canister wall so the reduced wall thickness has little effect on loading conditions.

4.4.3 *Handling and Lifting*

As noted, the compression loads were governed by stress and the same is true for lifting. The relative strength of the HCC is 1 to 2.8 that of the standard design. The tensile load limits for either are greater than 50,000 pounds. The canister top head is currently limited to 14,500 pounds so both designs are acceptable.

Handling of empty canisters with a fork lift exposes them to a combination of weight and clamping forces. During clamping, the standard canister remains elastic, deflects only 1/32" when clamped, and returns to original shape when clamping force is removed. By comparison, the HCC also remains essentially elastic, but deflects ¼" when clamped, and maintains an imperceptible and structurally insignificant 0,002 inch deflection when the clamping force is removed. This residual deflection is due to very localized regions in the canister wall, at the edges of the clamp, approaching and reaching yield stress. This is a secondary stress condition, as the core of the vessel wall is elastic. A lower clamping pressure (10% to 20% reduction) would be recommended for the HCC if the ¼ inch deformation during clamping were optically undesirable.

4.4.4 *Dent and Puncture Resistance*

Different handling steps can impose loads that might cause denting of the canister, particularly prior to filling. Wall thickness is significant and leads to nearly an order of magnitude difference in resistance between the two designs. The HCC was evaluated with a single point of support against the full weight of the canister and proved to have acceptable performance. This condition should bound other scenarios where multiple contacts are involved.

The puncture resistance of filled canisters was not considered relevant and was not evaluated. It is likely that an empty canister would either deform or push away from a force large enough to puncture the wall. This would probably be even more likely in the case of the thinner walled canister. Assuming a dynamic force capable of causing puncture were present, the puncture resistance of the empty canisters was shown to be proportional to thickness raised to the 1.5 power. Thus, a standard canister is 4.9 times more resistant to puncture than the HCC.

4.5 Decontamination

As discussed in the results section, the overall effect of the thickness reduction is minimal with respect to decontamination. The perforation resistance of the HCC after decontamination would be reduced by ~1.5%, which is not significant in terms of canister integrity.

4.6 Corrosion

No stress corrosion cracking (SCC) was found when thinner 304-L small scale canister samples were subjected to environmental conditions similar to previous standard canister testing. Assuming similar residual stresses from fabrication between the two designs, the SCC behavior of the current design should be similar or identical to that of the HCC.

5.0 Recommendations

This study did not address the issue of radiation shielding. Calculations showing that the HCC falls within the stated criteria for the facility would be necessary to document this requirement.

While the results for corrosion testing were positive, not all extreme conditions were evaluated. The specific conditions effecting SCC include salt exposure, tensile stress/strain, temperature, and moisture. The moisture available can be limited by promptly sealing the canister after the pouring operation. This is the normal procedure in DWPF and if strictly followed can ensure SCC resistance even, if other factors are higher than expected.

6.0 References

1. RPT-5539-ME- 0004, "Higher Capacity Canister (HCC) Drop Test Literature Search and Engineering Evaluation," S. Shiraga - Energy Solutions.
2. WSRC-IM-91-116-0 Rev 9, "DWPF Waste Form Compliance Plan," K. A. Hauer, 2006
3. HLW-DWPF-TTR-2011-0002 Rev 0, "Evaluation of Requirements for the DWPF Higher Capacity Canister (HCC)," Jan 2011
4. SRNL-RP-2011-0026 Rev 0, "Task Technical and Quality Assurance Plan for the Evaluation of the Defense Waste Processing Facility Higher Capacity Canister," April 2011.
5. DPST-78-380, "Thermal Analysis of DWPF Canister Processing," M. H. Tennant.
6. SRNL-STI-2011-00546, "Computer Modeling of High-Level Waste Glass Temperatures Within DWPF Canister During Pouring and Cool Down." J. W. Amorosa, September 2011.
7. DPST-87-801, "Canister and Glass Temperatures During Filling and Cool Down," R. E. Edwards, 1987.
8. SRNL-L4221-2011-00015, "Thermal Modeling of DWPF Canister Using Current and Proposed Thin Wall Designs," M.R. Kesterson, Nov 2011.
9. Calculation M-CLC-A-00466, "Structural Evaluation of DWPF Canister During Cool Down," J. M. Jordan.
10. M-SPP-S-00067 Revision 5, Specification for Procurement of DWPF Canisters, Tapered Plugs, and Plug Welds, D. J. Hutsell.
11. Energy Solutions Drawing # DW-5539-ME-0800-01, "DWPF Melter-2 HCC Design Canister Assembly".
12. WSRC-RP-91-0360, "Wall Thickness and Canisters for DWPF Test Program," J. R. Harbour, M. J. Plodinec.
13. WSRC-IM-91-116-008 Rev 3,"DWPF Canister Procurement, Control, Drop Test, and Closure," March 2006.
14. Calculation T-CLC-S-00295, "Structural Evaluations of DWPF Canister at 0.13 Inch Wall Thickness," Rev 1, C. A. McKeel.
15. DPST-87-784, Canister Decontamination Chamber #1 Operability Test Results," V. E. Magoulas.
16. DPST-83-749, "DWPF Canister Corrosion Experiments," C. A. Langton.
17. WSRC-TR-95-0455, "Salts in the Interior of DWPF Canistered Waste Form," M. K. Andrews, J. R. Harbour, D. T. Herman, C. A. Cicero, N. E. Bibler.
18. WSRC-TR-92-260, "Inorganic Analysis of Volatilized and Condensed Species within Prototypic Defense Waste Processing Facility (DWPF) Canistered Waste," C. M. Jantzen.
19. WSRC-TR-95-0455, "Analytical Results and Path Forward for Yellow Deposits Found in FA-13 Canisters," M. K. Andrews, J. R. Harbour, D. T. Herman.
20. WSRC-TR-95-0222, " A Technical Basis to Relax the Dew Point Specification for the Environment in the Vapor Space of the DWPF Canisters," M. R. Louthan.
21. WSRC-MS-95-0244, "Dew Point, Internal Gas Pressure and Chemical Composition of the Gas Within the Free Volume of the DWPF Canistered Waste Forms," J. R. Harbour.
22. WSRC-TR-92-308 Rev. 1, "Chemical Compatibility of DWPF Canistered Waste Forms," J. R. Harbour.
23. DPST-81-897, "Steady State Temperature in the DWPF Canister," D.R. Boyd to D. J. Pellarin, Nov 1981.
24. WSRC-RD-92-2 Rev. 1, "Method of Calculation of Heat Generation Rates for DWPF Glass," M. J. Plodinec.

25. WSRC-TR-93-520, “Glass Temperatures in Free Standing Canisters,” B, J. Hardy, and S. J. Hensel.
26. SRNL-L4000-2012-00006, “High Capacity Canister Stress Corrosion Cracking Evaluation”, E. G. Estochen
27. DPST-83-767-TL, “DWPF Canister Decontamination”, Memo from W. N. Rankin, August 1983.
28. SRNL-L3100-2011-0133 Rev. 0, “Chemical Composition Analysis of the Melter Feed Tank Batch 558 Sample”, F. C. Johnson, D. R. Click.

Distribution:

S. L. Marra, 773-A
J. W. Amoroso, 999-W
T. B. Brown, 773-A
E. G. Estochen, 773-A
S. D. Fink, 773-A
C. C. Herman, 773-A
D. T. Herman, 735-11A
E. N. Hoffman, 999-W
K. J. Imrich, 773-A
J. M. Jordan, 704-2H
M. R. Kesterson, 703-41A
D. H. McGuire, 999-W
C. A. McKeel, 730-A
D. H. Miller, 999-W
D. K. Peeler, 999-W
F. M. Pennebaker, 773-42A
M. E. Stone, 999-W
W. R. Wilmarth, 773-A
J. M. Bricker, 704-27S
J. S. Contardi, 704-56H
T. L. Fellinger, 704-26S
E. J. Freed, 704-S
J. M. Gillam, 766-H
B. A. Hamm, 766-H
E. W. Holtzscheiter, 704-15S
R. C. Hopkins, 704-24S
J. F. Iaukea, 704-27S
D. W. McImoyle, 766-H
J. W. Ray, 704-S
P. J. Ryan, 704-30S
H. B. Shah, 766-H
D. C. Sherburne, 704-S
J. A. Crenshaw, 703-46A
P. R. Jackson, DOE-SR, 703-46A
K. H. Subramanian, 241-156H
Records Administration (EDWS)